Optimization of synthesis conditions of gold nanoparticlespolydimethylsiloxane composite for ultrasound generation

Qing Wang, Jia Zhou, Xiaohan Wu, Antoine Riaud

Optimization of synthesis conditions of gold nanoparticles – polydimethylsiloxane composite for ultrasound generation

Qing Wang [1], Jia Zhou [1,*], Xiaohan Wu [2] and Antoine Riaud [1,*]

[1] State Key Laboratory of ASIC and System, School of Microelectronics, Fudan University, Shanghai 200433, China

[2] ALD/MLD Technology and Functional Device Research Team, School of Microelectronics, Fudan University, Shanghai 200433, China

* Corresponding authors

E-mail: antoine_riaud@fudan.edu.cn, jia.zhou@fudan.edu.cn

ABSTRACT

Gold nanoparticles (AuNP) - polydimethylsiloxane (PDMS) composites are promising materials for photoacoustic (PA) generation owing to their high thermal dilatation coefficient, small thermal capacity and acoustic impedance close to water. Solvent choice during AuNP synthesis can dramatically enhance the optical absorption of the composite, but there is no unified picture on this parameter. Here we test the optical absorbance and photoacoustic amplitude of AuNP-PDMS composites synthesized in five common solvents (acetone, methanol, ethanol, isopropanol, water). We find that photoacoustic signals from water and acetone yield small and sharp acoustic displacement peaks whereas alcohols yield larger steps-like downward displacements, which translates in a different Grüneisen parameter between the two groups. Furthermore, our experiments show that composites synthesized in isopropanol instead of ethanol showed a homogeneous surface, a nearly total optical absorption on a narrow bandwidth, and boosted the photoacoustic amplitude by up to 20%.

Keywords: PDMS functionalization, ultrasound generation, gold nanoparticles, photoacoustic effect, optical absorption

1 INTRODCTION

Polydimethylsiloxane (PDMS)[1-3] is a promising material for photoacoustic (PA) generation owing to its high thermal dilatation coefficient, small thermal capacity and acoustic impedance close to water. However, PDMS is a transparent material, which

limits its performance as a photoacoustic conversion layer. The optical absorption of PDMS is often increased using either opaque materials (carbon nanotubes[4, 5], graphene[6], carbon soot [7, 8],carbon black[9, 10], carbon fiber[11]) or bandwidth specific materials (such as gold[12, 13] and silver nanoparticles[14]). These narrowband absorbers enable emission and reception of ultrasonic signals in an all-optical fashion[1], but are limited by a lower conversion coefficient than black materials, which in turn requires thicker absorbing layers that restricts the ultrasonic bandwidth.

In 2007, Zhang et al.[15] pioneered a top-down synthesis approach where a slab of cured PDMS is immersed in a tricholoauric acid (TCA) aqueous solution. The PDMS contains left-over silicon hydride Si-H groups that reduce the TCA into nanoparticles. This yields a thin layer (~ 2 μm) of nanoparticles embedded in a PDMS matrix. Switching solvent from water to ethanol further improves the absorbance from 27%[15] to 91%[1] with a 30 MHz bandwidth, yielding a multimodal generation layer competitive with black materials.

The dramatic improvement obtained after switching solvents suggests that, beyond TCA[16] and PDMS curing agent concentrations[15], the solvent plays a key role in the composite absorbance. This is down to several factors:

First, the solvent alters the physical structure of PDMS by irreversible swelling [[16-20]].

Second, from mass transfer considerations, the solvent (i) brings the $AuCl_4^-$ anions inside the PDMS[15] where they react with the Si-H groups, (ii) it extracts the curing agent from the PDMS[17] and (iii) some solvents can swell PDMS which can increase the depth of the diffusion layer of AuNP in the PDMS[21]. Finally, from a reaction

perspective, the right solvent choice can displace the formation reaction equilibrium by eliminating the reaction byproducts Cl^- and H^+:

$$3\,\mathrm{Si{-}H} + 3/2\,H_2O + 2AuCl_4^- \rightarrow 3/2\,\mathrm{Si{-}O{-}Si} + 2Au + 8Cl^- + 6H^+$$

In summary, the choice of solvent has a multidimensional effect on the synthesis of AuNP-PDMS composites, and it is unclear if further adjusting the solvent would result in a better photoacoustic generation performance. In this study, we test five common solvents (acetone, methanol, ethanol, isopropanol, water) at a range of TCA concentrations (from 0.003 mol L^{-1} up to 0.018 mol L^{-1}, that is 0.1% (m/v) up to 0.7% (m/v)). The composite is evaluated in terms of uniformity, absorbance and photoacoustic generation amplitude with a 520 nm pulsed laser diode. We then combine our data in a linear model to predict the absorbance depending on the TCA concentration, the solvent polarity, solvent pKa, the Hildebrandt solubility parameter between the solvent and PDMS, and the swelling coefficient:

$$S = \frac{W_s - W_b}{W_b}, \quad (1)$$

where W_s is the weight of Au-free PDMS sample after swelling by each solvent and W_b is the weight of each Au-free PDMS sample before swelling process. We find that photoacoustic signals from water and acetone yield small and sharp acoustic displacement peaks whereas alcohols yield larger steps-like downward displacements, which translates in a different Grüneisen parameter between the two groups. We also note that using isopropanol instead of ethanol yields a more uniform photoacoustic conversion layer with twice the absorbance and a 20% larger photoacoustic amplitude at equal laser power.

2 MATERIALS AND METHODS

2.1 Materials

Sylgard® 184 elastomer kit including base polymer and the curing agent for PDMS fabrication was purchased from Dow Corning Inc., USA. TCA trihydrate ($HAuCl_4 \cdot 3H_2O$, 99.9%) was purchased from Sigma-Aldrich, Shanghai, China. Methanol, ethanol, isopropanol and acetone were provided by Sinopharm Chemical Reagent Co., Ltd. All other chemicals were obtained commercially and without purification.

2.2 Fabrication of PDMS and PDMS modification by AuNP

AuNP were prepared based on the recipe of SadAbadi et al[22], where ethanol was replaced by other solvents. Briefly, PDMS substrates were firstly prepared by mixing the base and the curing agent at a weight ratio of 10:1 with mechanical stirring. The mixture was homogenized in an ice-cooled ultrasonic bath for 30 min. To test various compositions and solvents, the mixture was split in several 800 μL samples that were poured glass test tubes with 15 mm of diameter and 5 mm of height. The mixture was degassed in a vacuum chamber for 30 min. Finally, the samples were cured at 70 ℃ in an oven overnight. For future reference, the composites prepared in methanol will referred as “methanol samples”, those in acetone as “acetone samples” and so on.

Methanol, ethanol, acetone, and water samples were prepared with the same synthesis method. For each of the five solvents, we prepared a 0.018 mol L^{-1} stock solution of TCA. The solutions were then screened with a 0.22 μm filter and diluted to 0.003, 0.008, 0.013, 0.015 mol L^{-1}, that is 0.1% (m/v) up to 0.7% (m/v). To prepare the diluted solutions. 300 μL of TCA solutions were poured in the test tubes containing cured

PDMS. To prevent evaporation, the bottles were then sealed by wrapping them in parafilm and capped by an oak stopper. After incubating for 48 h, the synthesized nanocomposites were taken out and rinsed with water and dried with nitrogen.

2.3 Characterization

The optical absorption of the samples was measured with a UV-Vis spectrometer (TU-1810). The morphology and geometric structure of the nanocomposites were observed using optical microscope (OM, BX53M, Olympus). A digital camera was used to take unmagnified images, compared with images obtained by OM with 100× magnification. The optical absorption of the solvent samples is then measured with a UV-Vis spectrophotometer and the Au-free PDMS is taken as reference sample.

The photoacoustic vibrations of solvent samples with 0.015 $mol.L^{-1}$ TCA concentration irradiated with a 129 ns pulse with 1.5 W peak power (attenuated to 0.3 W after the 10× objective) are measured with a home-made heterodyne Mach-Zehnder laser vibrometer[23, 24].

3 RESULTS

3.1 Optical microscopy imaging of the PDMS composite surface

OM photographs of the solvent samples with various TCA concentrations are shown in Figure 1, with unmagnified images presented in the inset. For a given solvent, the purple-red color of the samples becomes darker with increasing TCA concentration. For a given TCA concentration, color depth of samples gradually increases in the order of water, acetone, methanol, ethanol, and isopropanol samples. Previous studies[12] suggest that darker samples indicate that more TCA successfully form AuNP.

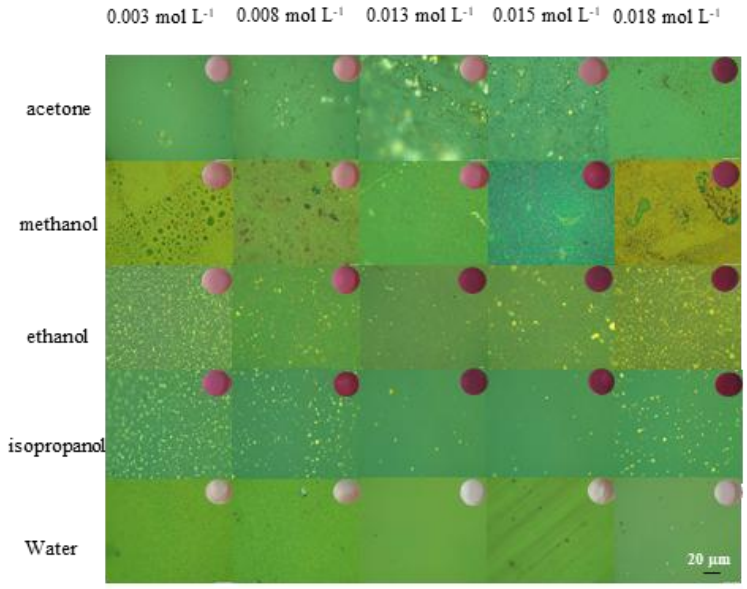

Figure 1. OM images of nanocomposites with 100× magnification. Vertical direction including acetone, methanol, ethanol, isopropanol, and water samples, horizonal direction where TCA solution ranged from 0.003 to 0.018 mol L^{-1}. Inset: images of digital camera for 25 samples. Scale bar: 20 μm.

OM images show large yellow agglomerates (believed to be gold microparticles) on most samples except water. These large yellow particles are unlikely to yield an absorption peak at 532 nm and PA signals with a 520 nm laser and are therefore regarded as a side-product. To quantify the size and amount of Au microparticles on the surface of PDMS, we use Photoshop® to count the percentage of yellow in each sample photograph. The results are shown in Figure 2. Interestingly, the amounts of yellow particles depending on the TCA concentration follows a non-monotonic *N*-shaped curve (divided in 3 segments denoted I, II, III) regardless of the solvent. Scarano et al, who reported a similar trend for water samples [16], offered a kinetic interpretation for this phenomenon. When TCA is scarce, the gold particles are

formed slowly which favors large microscopic aggregates whereas at higher TCA concentration the gold reduction would proceed faster and yield nanoparticles, thus the dip in yellow percentage. Scarano et al. did not investigate larger concentrations, but indicated that using ethanol to deplete the PDMS from silicon hydride groups and then adding more TCA yield large particles again. Therefore, the upper trend at large TCA concentration may be due to the exhaustion of the Si-H groups in the PDMS (consumed to make AuNP or dispersed in the solvent).

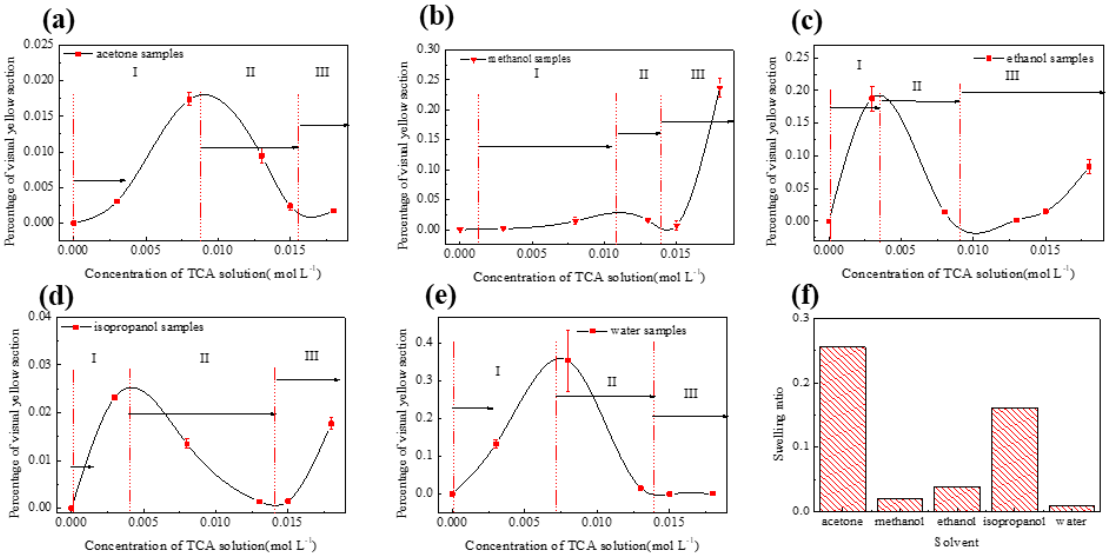

Figure 2. Percentage of visual yellow section to surface area of Au-free PDMS solvent samples and swelling ratio of each solvent (a) Acetone. (b) Methanol. (c) Ethanol. (d) Isopropanol. (e) Water. (f) Swelling ratio of solvent to PDMS matrix.

We then evaluate the size distribution of the microparticles on the samples surface. The particle size distribution of existing composites (ethanol 0.013 mol L^{-1} [1] and water 0.013 mol L^{-1} [15]) are compared with the best sample of this study (isopropanol 0.015 mol L^{-1}) in Figure 3 (the other samples are available in SI). While the ethanol samples have dozens of microparticles, the isopropanol and water samples have only

submicrometric particles. Therefore, the isopropanol sample combines the high absorbance of ethanol samples with the excellent homogeneity of water samples, which is essential for micro-photoacoustic applications such as fiber-optic photoacoustic transducers or integration in microfluidic chips.

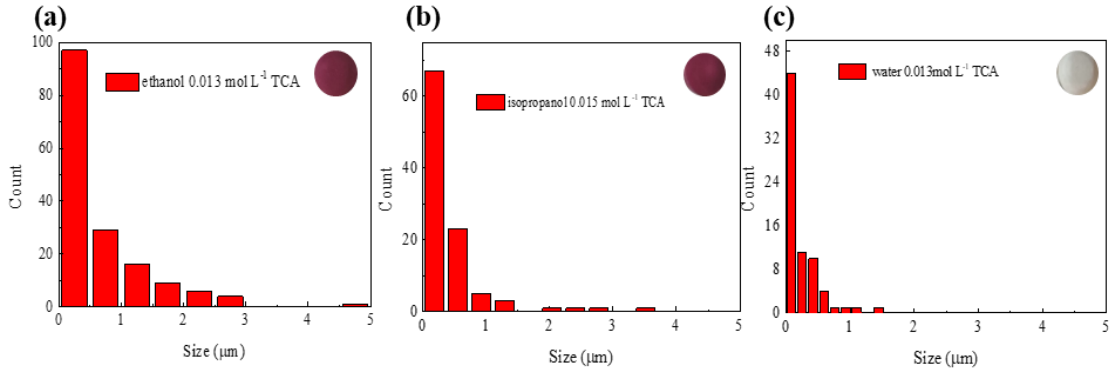

Figure 3. The amount of visible yellow particles. (a) Ethanol samples with 0.013 mol L^{-1}. (b) Isopropanol sample with 0.015 mol L^{-1}. (c) Water sample with 0.013 mol L^{-1}. Inset: images of digital camera of 0.013 mol L^{-1} ethanol, 0.015 mol L^{-1} isopropanol, 0.013 mol L^{-1} water samples.

3.2 Optical absorbance

The relative absorption spectra at 0.015 mol L^{-1} TCA concentration samples are shown in Figure 4. Maximum absorption peaks are at 540±10 nm. Red-shifts are observed at the methanol and water samples of 2 nm and 10 nm, respectively. The absorbance increases from 20% (water) up to 95% (isopropanol). Half width at half maximum (HWHM) are measured and the isopropanol sample exhibits the narrowest absorbance peak.

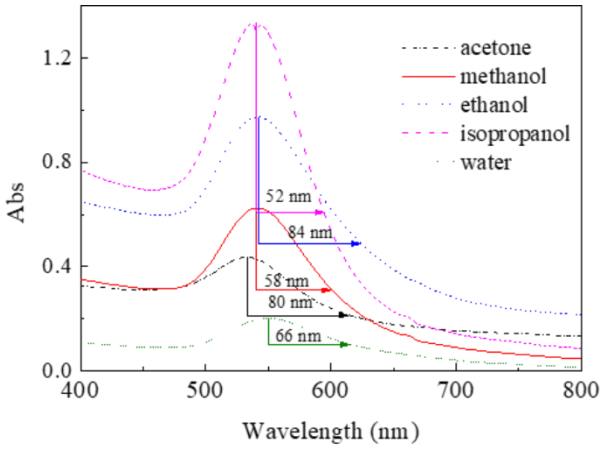

Figure 4. UV-Vis absorption spectrums of the five solvent samples at 0.015 mol L^{-1} of TCA concentration.

3.3 PA signal generation

The generated PA signals are plotted in Figure 5. Unlike most experiments measuring the acoustic pressure, we record the displacement of a thin reflective mylar foil placed under the generation layer upon irradiation by the laser pulse. To avoid acoustic reflections, an Au-free PDMS slab is placed under the mylar film. Our interferometer displays the surface displacement, which is positive when the mylar is moved away from the vibrometer by the thermal dilatation of the generation layer. We found that acetone and methanol samples were noisier than isopropanol, water and ethanol samples. The 6.4 nm jump height (PA amplitude) of the isopropanol sample is 3 times higher than for the water sample (2.0 nm) and 20% higher than that the ethanol sample (5.1 nm). The peak to peak PA amplitude increases with the order of acetone, water, methanol, ethanol, and isopropanol. Water and acetone, on the one hand, and alcohols (methanol, ethanol, isopropanol) on the other exhibit markedly different waveforms. While the former jump promptly back in place, the alcohol samples displacement remains large even long after the pulse. Careful examination of the

methanol samples reveals the coexistence of two characteristic relaxation times, a short one (similar to water), and a long one, as for ethanol and isopropanol. At the time of writing this paper, we are still investigating the reasons for this difference. We also note that we saw no evidence of damage on any of the generation layers.

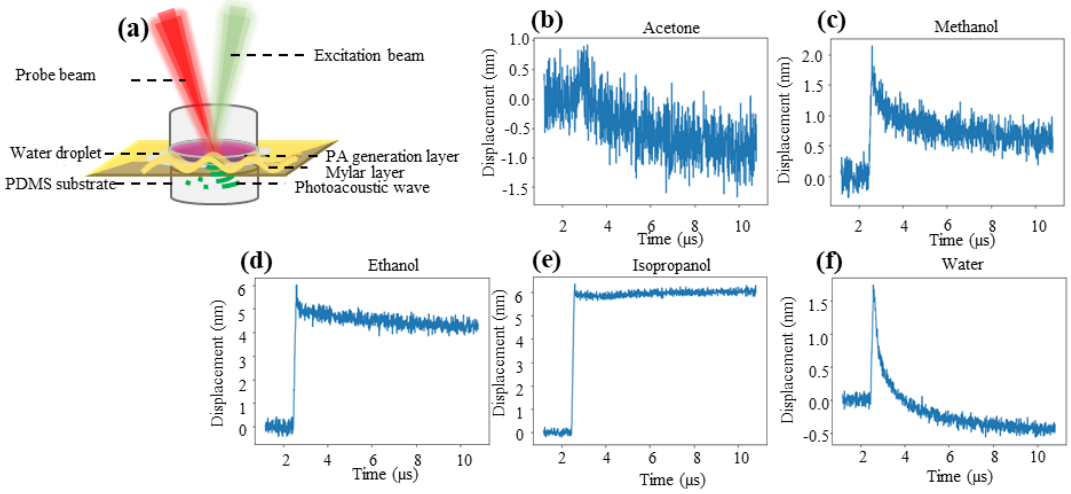

Figure 5. (a) The schematic diagram of PA generation experimental set-up. (b) PA waveform of acetone sample. (c) PA waveform of methanol sample. (d) PA waveform of ethanol sample. (e) PA waveform of isopropanol sample. (f) PA waveform of water sample. Condition: 129 ns pulse with 0.3 W peak power near samples, TCA concentration was 0.015 mol L^{-1}, The laser strikes the sample at t = 2.4 μs, causing thermal dilatation that results in sudden sample displacement.

DISCUSSION

Our experiments show that using isopropanol as a solvent yields homogeneous samples with enhanced light absorption and 20% superior photoacoustic amplitude at equal laser power. In the following discussion, we first clarify whether the enhanced performance comes from a modification of the PDMS bulk (such as swelling) or from the superior light absorption. We then interpret this optimal solvent choice using a

linear model and propose a simple reaction mechanism to explain the enhancement.

4.1 Cause of the enhancement

Theoretically, the PA displacement amplitude u is given by[1]:

$$u = \Gamma \mu_a \varphi_i, \tag{2}$$

with Γ the Grüneisen parameter, μ_a the optical absorption coefficient and φ_i the incident light fluence. The absorbed power flux $\varphi_{abs} = \mu_a \varphi_i$ can be deduced from the absorbance $Abs = \log_{10}\left(\frac{\varphi_i}{\varphi_t}\right)$ by using the power conservation $\varphi_i = \varphi_t + \varphi_{abs} + \varphi_r$ where the reflected power φ_r is negligible for AuNP-PDMS composites[25]. This yields $\mu_a \approx 1 - 10^{-Abs}$ and the theoretical relation:

$$u \approx \Gamma \varphi_i (1 - 10^{-Abs}), \tag{3}$$

This theoretical relation is tested in Figure 6. We find that even though all the samples follow a common trend, there is a slope break between water/ketone and alcohol samples. This discontinuity combined with Eq. 3 suggests that higher PA of alcohol samples is at least in part due to an increase of Γ.

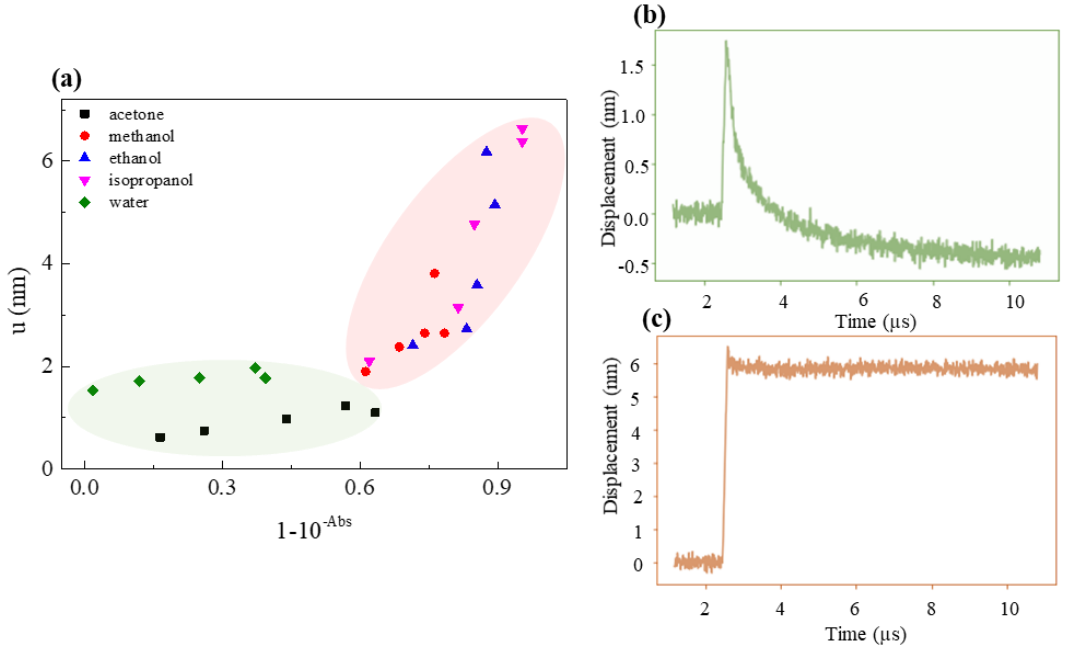

Figure 6. (a) Amplitude change with absorbance for 5 TCA concentrations in 5 different solvents (25 samples). Note: colored circles mark two types of PA waveform, water/ketone samples (green), alcohol samples (pink). (b) PA waveform of water sample. (c) PA waveform of isopropanol sample.

4.2 Effect of solvent characteristics on light absorption

Since absorbance and PA amplitude are closely related, we now study the effect of solvent parameters on the absorbance, bearing in mind that a similar law can be obtained for the PA amplitude. The absorption responses to the various solvent parameters at maximum wavelength 540 nm are studied in Figure 7 (a, b, c, d, e). The studied parameters include TCA concentration, solvent dipole moment, pKa of each solvent, Hildebrandt solubility parameter (reflect the molecular coherence of the solvent), and swelling value S, collected in Table 1. Figure 7 (a) shows a growth of optical absorption with increasing TCA concentration, indicating the more TCA molecules are reduced to form AuNP. At higher concentration, slight drop of the optical absorption appears except methanol and water samples. This result may be due to larger Au particles visible in the OM photographs which are not beneficial to improve absorbance at 540 nm. Figure 7 (b, c, d, e) show that no single factor in the solvent can explain the variations in absorber performance.

Table 1. Swelling degree, dipole moment, solubility parameter and pKa of five solvents

Solvents	S	dipole moment (D)	Solubility parameter ($cal^{1/2}$ $cm^{-3/2}$)	pKa

acetone	0.26	2.69	9.90	19.30
methanol	0.02	2.87	14.50	15.50
ethanol	0.04	1.69	12.90	15.90
isopropanol	0.16	1.66	11.50	16.50
water	0.01	1.85	23.4	14.00

However, a multilinear fit of these five factors shows a good fit with experimental results, as shown in Figure 7 (f). For this regression, the parameters are made dimensionless by comparison with water. The linear regression between PA amplitude and solvent properties are shown in SI with good linear relationship.

Table 2. parameters and regressed coefficients of the five solvents

Parameter	Normalized parameter	Regressed coefficient
Swelling (S)	$S' = \frac{S}{S_w} - 1$	$\theta_S = -0.001$
Dipole moment (q)	$q' = \frac{q}{q_w} - 1$	$\theta_q = -0.08$
Hildebrandt solubility parameter (h)	$h' = \frac{h - h_{pdms}}{h_w} - 1$	$\theta_h = -2.13$
Acidity constant (pKa)	$pKa' = \frac{pKa}{pKa_w} - 1$	$\theta_{pKa} = -2.64$
TCA concentration (C) *	$C' = \frac{C}{C_{Zhang}} - 1$	$\theta_C = 0.26$
Intercept (b)		b = -0.4

* C_{Zhang} = 0.013 mol L^{-1} is set as standard concentration based on previous studies.

$$\mu_a = b + \theta_C C' + \theta_S S' + \theta_q q' + \theta_h h' + \theta_{pKa}$$

The obtained linear regression coefficients are shown in Table 2 and Figure 8 (b). It suggests that more acidic solvents that have a solubility similar to PDMS favor the formation of AuNP, while swelling and solvent dipole moment are not related to the final absorption.

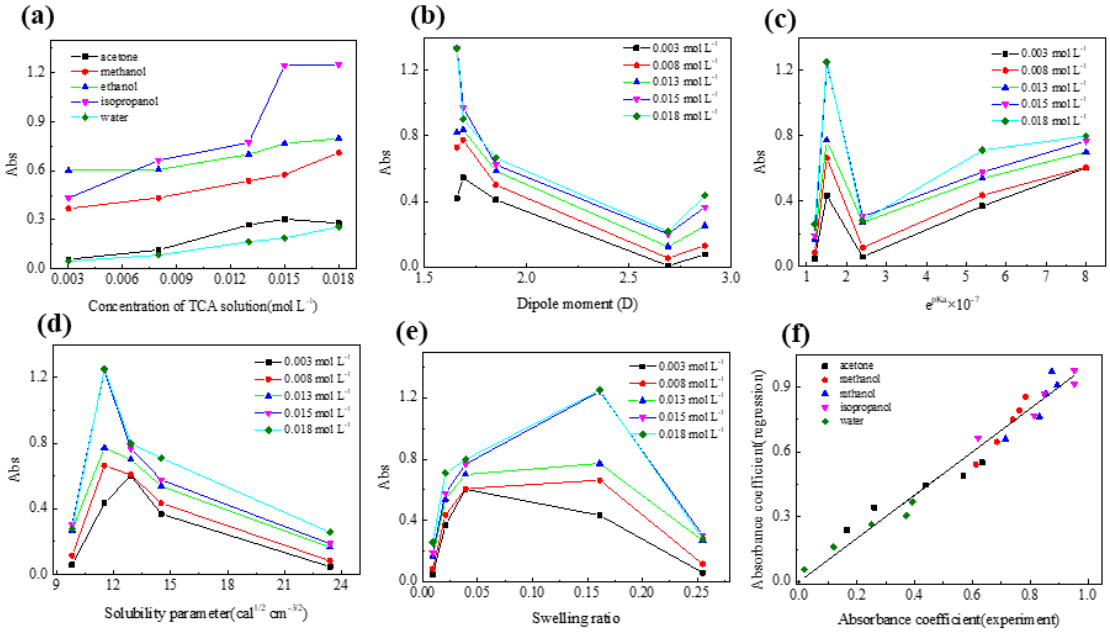

Figure 7. Relationship between solvent property and absorption, (a) Concentration of TCA solution at different solvents. (b) Solvent dipole moment. (c) pKa. (d) Solubility parameter. (e) Swelling ratio. (f) Comparison of linear model of absorption coefficient and experimental result.

Furthermore, we can reproduce the absorption ranking using only the two dominant factors, as shown in Figure 8 (a). The best material is in the lower-left corner. Each line represents theoretically equivalent materials. We get the ranking water < acetone < methanol < ethanol < isopropanol.

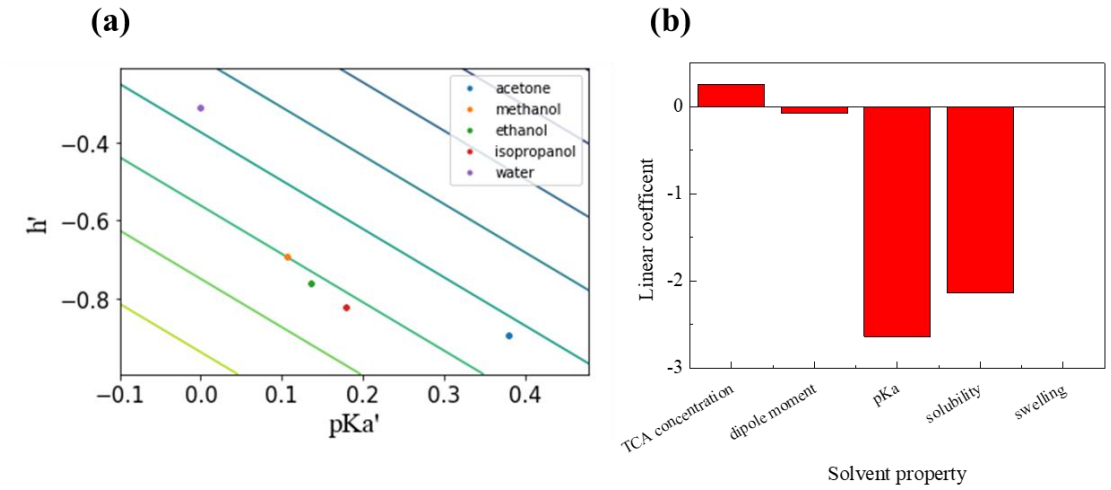

Figure 8. (a) Ranking of compounds based on the two major coefficients. (b) Comparison of linear coefficients of five solvent properties.

4.3 Postulated mechanism

The use of high Hilderbrandt solubility was previously discussed (in terms of permeation rates in PDMS) by SadAbadi et al., who argued that higher solvent permeation rates in PDMS accelerate the synthesis of thin AuNP films. Since the film is formed essentially at the surface of the PDMS, it is likely that more volatile solvents allow a faster extraction of the silicon hydride groups [22, 26]. Notwithstanding these solubility effects, we find that the pKa is the most important factor when comparing multiple solvents. While good bases would be able to accept the H^+ from the reaction, they do not eliminate the Cl^-. However, alcohols are well known to undergo nucleophilic substitution in acidic media:

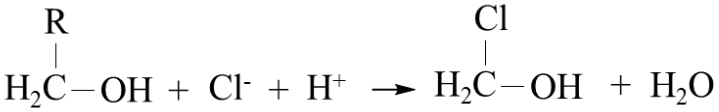

If such reaction was to happen, it would eliminate both products from reaction, thereby displacing the reaction equilibrium and favoring the formation of AuNP. This

could explain why alcohol synthesize darker samples than water and acetone. However, the difference in Grüneisen parameter is difficult to infer from chemistry and may require additional physical characterizations.

5 CONCLUSION

The synthesis of AuNP-PDMS composite for ultrasound generation is a complex multiphase reaction where the solvent has been shown to play a prominent role. Solvent effect on AuNP-PDMS synthesis was experimentally studied by measurements of morphology, optical absorption and photoacoustic generation. In the case of water, ethanol and isopropanol, AuNP were better dispersed on the surface of PDMS than for methanol and acetone. Comparing the PA amplitude and optical absorption, we found that the enhanced performance of AuNP-PDMS composites prepared in isopropanol was at least in part due to a different Grüneisen parameter between alcohol samples versus water and ketone ones. A simple linear model of optical absorption depending on the solvent dipole moment, swelling of PDMS, Hilderbrandt solubility and pKa then revealed that solubility and pKa are the dominant factors to determine the final optical absorption. Furthermore, these two parameters alone reproduce the ranking water < acetone < methanol < ethanol < isopropanol. Finally, we postulate that alcoholic solvents promote the formation of AuNP by consuming the H^+ and Cl^- side products through a nucleophilic substitution reaction. Our research demonstrates that the solvent choice is a key factor in the synthesis of nanoparticles on PDMS, and unveils that using isopropanol as a solvent instead of ethanol offers a 20% boost in photoacoustic amplitude.

ASSOCIATED CONTENT

Supporting information

Schematic diagram of PA generation experimental set-up, linear regression result of amplitude and solvent properties, size distribution diagrams for 25 solvent samples.

AUTHOR INFORMATION

Corresponding Author

State Key Laboratory of ASIC and System, School of Microelectronics, Fudan University, Shanghai 200433, China

E-mail: antoine_riaud@fudan.edu.cn, jia.zhou@fudan.edu.cn

Author Contributions

Antoine Riaud and Jia Zhou proposed the study. Qing Wang carried out experiments and characterizations, and prepared the figures for the manuscript. Antoine Riaud and Qing Wang analyzed data together. Xiaohan Wu provided instruments and guidance for the spectroscopy and absorbance measurements. All the authors wrote the manuscript together.

Notes

The authors declare no competing financial interest

ACKOWLEDGMENTS

This work was supported by National Natural Science Foundation of China with Grant No. 51950410582 and No. 61874033. LDV DATA analysis interface was provided by Miss Ting Xu in Fudan University. We are also grateful to be supported by associate Prof. Wu from School of Microelectronics at Fudan University.

ABBREVIATIONS

Au, gold; AuNP, gold nanoparticles; PDMS, polydimethylsiloxane; TCA, tetrachloroauric acid; PA, photoacoustic; S, swelling, LDV, heterodyne Mach-Zehnder Laser Doppler Vibrometer.

REFERENCES

1. Noimark, S.; Colchester, R. J.; Poduval, R. K.; Maneas, E.; Alles, E. J.; Zhao, T. R.; Zhang, E. Z.; Ashworth, M.; Tsolaki, E.; Chester, A. H.; Latif, N.; Bertazzo, S.; David, A. L.; Ourselin, S.; Beard, P. C.; Parkin, I. P.; Papakonstantinou, I.; Desjardins, A. E., Polydimethylsiloxane Composites for Optical Ultrasound Generation and Multimodality Imaging. *Advanced Functional Materials* **2018,** *28* (9).

2. Lee, T.; Baac, H. W.; Li, Q.; Guo, L. J. J. A. O. M., Efficient Photoacoustic Conversion in Optical Nanomaterials and Composites. **2018,** *6* (24), 1800491.1-1800491.30.

3. Baac, H. W.; Ok, J. G.; Hui, J. P.; Ling, T.; Chen, S. L.; Hart, A. J.; Guo, L. J. J. A. P. L., Carbon nanotube composite optoacoustic transmitters for strong and high frequency ultrasound generation. **2010,** *97* (23), 234104-234104.

4. Hyoung; Won; Baac; Jong; Ok; Taehwa; Lee; Nanoscale, J. J., Nano-structural characteristics of carbon nanotube-polymer composite films for high-amplitude optoacoustic generation. **2015**.

5. Baac, H. W.; Ok, J. G.; Maxwell, A.; Lee, K. T.; Chen, Y. C.; Hart, A. J.; Xu, Z.; Yoon, E.; Guo, L. J. J. S. R., Carbon-Nanotube Optoacoustic Lens for Focused Ultrasound Generation and High-Precision Targeted Therapy. **2012,** *2*, 989.

6. Hwan Lee, S.; Park, M. A.; Yoh, J. J.; Song, H.; Jang, E. Y.; Hyup Kim, Y.; Kang, S.; Seop Yoon, Y. J. A. P. L., Reduced graphene oxide coated thin aluminum film as an optoacoustic transmitter for high pressure and high frequency ultrasound generation. **2012,** *101* (24), p.1-4.

7. Deng, X.; Mammen, L.; Butt, H. J.; Vollmer, D. J. S., Candle Soot as a Template for a Transparent Robust Superamphiphobic Coating. **2012,** *335* (6064), 67-70.

8. Chang, W. Y.; Huang, W.; Kim, J.; Li, S.; Jiang, X. J. A. P. L., Candle soot nanoparticles-polydimethylsiloxane composites for laser ultrasound transducers. **2015,** *107* (16), 1713.

9. Buma, T.; Spisar, M.; O'Donnell, M. J. A. P. L., High-frequency ultrasound array element using thermoelastic expansion in an elastomeric film. **2001,** *79* (4), 548-550.

10. Nomada, H.; Morita, K.; Higuchi, H.; Yoshioka, H.; Oki, Y. J. T., Carbon–polydimethylsiloxane-based integratable optical technology for spectroscopic analysis. **2017**, 428-432.

11. Hsieh, B. Y.; Kim, J.; Zhu, J.; Li, S.; Zhang, X.; Jiang, X. J. A. P. L., A laser ultrasound transducer using carbon nanofibers–polydimethylsiloxane composite thin film. **2015,** *106* (2), 8.

12. Wu, N.; Tian, Y.; Zou, X.; Silva, V.; Chery, A.; Wang, X. J. J. o. t. O. S. o. A. B., High-efficiency optical ultrasound generation using one-pot synthesized polydimethylsiloxane-gold nanoparticle nanocomposite. **2012,** *29* (8), 2016-2020.

13. Zou, X.; Wu, N.; Tian, Y.; Wang, X. J. O. E., Broadband miniature fiber optic ultrasound generator. **2014**.

14. Zhao, H.; Hasi, W.; Bao, L.; Liu, Y.; Han, S.; Lin, D. J. J. o. R. S., A silver self‐assembled monolayer‐decorated polydimethylsiloxane flexible substrate for in situ SERS detection of low‐abundance molecules. **2018,** *49* (9), 1469-1477.
15. Zhang, Q.; Xu, J. J.; Liu, Y.; Chen, H. Y. J. L. o. A. C., In-situ synthesis of poly(dimethylsiloxane)–gold nanoparticles composite films and its application in microfluidic systems. **2008,** *8*.
16. Scarano, S.; Berlangieri, C.; Carretti, E.; Dei, L.; Minunni, M. J. M. A., Tunable growth of gold nanostructures ata PDMS surface to obtain plasmon rulers with enhanced optical features. **2017**.
17. Lee, J. N.; Park, C.; Whitesides, G. M. J. A. C., Solvent Compatibility of Poly(Dimethylsiloxane)-Based Microfluidic Devices. **2004,** *75* (23), 6544-6554.
18. Rumens, C. V.; Ziai, M. A.; Belsey, K. E.; Batchelor, J. C.; Holder, S. J. J. J. o. M. C. C., Swelling of PDMS networks in solvent vapours; applications for passive RFID wireless sensors. **2015,** *3* (39), 10091-10098.
19. Kim, M. M.; Huang, Y.; Choi, K.; Hidrovo, C. H. J. M. E., The improved resistance of PDMS to pressure-induced deformation and chemical solvent swelling for microfluidic devices. **2014,** *124* (jul.), 66-75.
20. Kim, B. Y.; Hong, L. Y.; Chung, Y. M.; Kim, D. P.; Lee, C. S. J. A. F. M., Solvent-Resistant PDMS Microfluidic Devices with Hybrid Inorganic/Organic Polymer Coatings. **2010,** *19* (23), 3796-3803.
21. Jeremy; R.; Dunklin; Gregory; T.; Forcherio; Keith; R.; Berry; Materials, J. J. A. A.; Interfaces, Asymmetric Reduction of Gold Nanoparticles into Thermoplasmonic Polydimethylsiloxane Thin Films. **2013,** *5* (17), 8457-8466.
22. Hamid; SadAbadi; Simona; Badilescu; Muthukumaran; Packirisamy; Rolf; Nanotechnology, W. J. J. o. B., PDMS-Gold Nanocomposite Platforms with Enhanced Sensing Properties. **2012,** *8* (4), 539-549.
23. Royer, D.; Dieulesaint, E.; Martin, Y. In *Improved Version of a Polarized Beam Heterodyne Interferometer*, IEEE 1985 Ultrasonics Symposium, 1985.
24. Royer, D.; Dieulesaint, E. In *Optical Detection of Sub-Angstrom Transient Mechanical Displacements*, IEEE 1986 Ultrasonics Symposium, 1986.
25. Dunklin, J. R.; Forcherio, G. T.; Berry, K. R.; Roper, D. K. J. A. M.; Interfaces, Asymmetric Reduction of Gold Nanoparticles into Thermoplasmonic Polydimethylsiloxane Thin Films. **2013,** *5* (17), 8457-8466.
26. Lee; Jessamine; Ng; Park; Cheolmin; Whitesides; George; Chemistry, M. J. A., Solvent Compatibility of PoIy (dimethylsiloxane)-Based Microfluidic Devices. **2003**.